Chemical Durability of Phosphate Laser Glasses Polished with Pitch, Pads, or MRF

Introduction

Large, high-power laser systems are currently under construction; such systems include the National Ignition Facility (NIF) at Lawrence Livermore National Laboratory (LLNL),[1] the LMJ laser at CEA in France, and the OMEGA EP at LLE.[2] These new lasers will require large amounts of neodymium phosphate laser glass, which is known to be sensitive to water.[3] When improperly handled or exposed to too much humidity, phosphate glass surfaces may cloud—a result of increased surface roughness due to chemical reactions. Smooth surfaces are required for such lasers (for example, a 2- to 10-Å-rms roughness level is specified for the NIF[1]); rougher surfaces cause scatter, which can result in intensity modulation in the laser beam, leading to damage to downstream optics and "(increased) fluence on the spatial-filter pinholes."[1] Transmission loss also causes output energy loss, significantly reducing performance. Thus the chemical durability of the laser glass used is of great importance to its fabrication, storage, cleaning, and handling.

Cast Hoya LHG8 phosphate glass, which is made in small individual batches, has been handled and used for over 25 years at LLE in the OMEGA laser system. It was found that a 50/50 glycol and water mixture was required to cool the fine-ground barrels of laser rods without erosion of the LHG8 composition,[3,4] but no other chemical durability problems with the polished faces of cast LHG8 rods and disks were encountered. The new lasers will use phosphate glass manufactured by a continuous melting process[5] developed by LLNL for the NIF laser. In addition to the LHG8 composition used in OMEGA, a new phosphate glass composition, Schott LG770, will be used in the NIF. Changes in manufacturing technique and composition may affect chemical durability.

Previous work at LLNL[6] has shown the continuously melted LG770 to be less resistant to attack by water than the continuously melted LHG8. The quality of the surface finish (between grinding, inspection polishing, and optical finishing) was found to affect dramatically the rate at which the glasses weathered. Both compositions were shown to be sensitive to residual abrasives when they were allowed to dry on the surface after polishing,[6] which is a known effect on surfaces of low-durability glass.[7] The limited use of scrubbing with aqueous detergent solutions was specified for removing protective coating residues from phosphate glass surfaces after storage.[8]

After finishing, three practical issues for preserving the surface quality of phosphate glass are handling, storage, and sensitivity to cleaning. This work focused on determining how resistant each composition was to various levels of humidity; whether or not the manufacturing method (casting versus continuous melting) affected humidity resistance; what effect the surface-finishing process had on resistance to humidity or response to cleaning; the effect of periodic, gentle wiping during storage; and the effect of aggressive aqueous cleaning (of the sort typically used before installing optics into laser systems) on both "good" surfaces and degraded ones.

Experimental Design

The following subsections summarize our general experimental design. Samples of each glass type were processed using three different finishing techniques: pitch polishing, pad polishing, or magnetorheological finishing (MRF). Samples were stored in chambers at four different controlled humidities at 22°C for 14 weeks. Half of the samples underwent a gentle weekly wiping during storage. A total of 48 samples with 80 prepared surfaces were monitored. The distribution of the samples is given in Fig. 100.35, where sample ID's are listed in bold and sides prepared with different polishing protocols are labeled as S1 and S2. For example, sample 13C denotes a continuously melted LG770 part intended for storage at 38% RH (relative humidity) that has undergone the gentle weekly wiping. Surface S1 of the part had been pitch polished, while surface S2 had been pad polished. Samples used to illustrate trends discussed extensively in this article are highlighted in Fig. 100.35 in gray. Surface microroughness analyses and power spectral density analyses were performed, and the visual appearance of each sample was monitored. After 14 weeks, samples stored in high humidity underwent a thorough visual and microscopic inspection before undergoing two aqueous

cleanings by technicians in the optics manufacturing facility at LLE. Some of these high-humidity samples were cleaned with water alone, and some with water and detergent. After each cleaning, these samples were measured and inspected again.

1. Sample Preparation

Testing was performed on identically processed, handled, and stored samples of cast LHG8 (designated C-LHG8), continuously melted LHG8 (designated CM-LHG8), and continuously melted LG770 (designated CM-LG770). Samples were nominally 25 mm × 25 mm × 5 mm. The samples of C-LHG8 came from in-house stock, and the samples of CM-LHG8 and CM-LG770 came from LLNL. Samples of C-LHG8 and CM-LHG8 underwent pitch polishing, rotational magneto-rheological finishing (MRF), and raster MRF. MRF is a finishing method that involves polishing a surface by moving it through a ribbon of a magnetic fluid that contains abrasives.[9] Samples of CM-LG770 underwent pitch polishing, pad polishing, rotational MRF, and raster MRF. Pitch polishing was done in-house on a 36-in. continuous polishing (CP) machine, with Gugolz #82 pitch, using an aqueous slurry containing Cerox 1663 cerium oxide. Samples were cleaned with acetone after pitch polishing. Pad polishing (on CM-LG770 only) was done by an outside vendor in a double-sided process using cerium oxide and pads. These parts were used "as-received." MRF using both rotational and raster modes of processing was done in-house on a QED Technologies Q22-Y machine using an experimental ZrO_2-based MR fluid.[10] For rotational MRF, samples were polished by rotating the surfaces of the spindle-mounted parts as they were moved through the magnetic ribbon. For raster MRF, the parts were translated without rotation through the ribbon in a raster fashion. MRF was performed on previously pitch- or pad-polished surfaces, with at least 0.2 μm of material uniformly removed. After MRF, samples were wiped with water, followed by acetone.

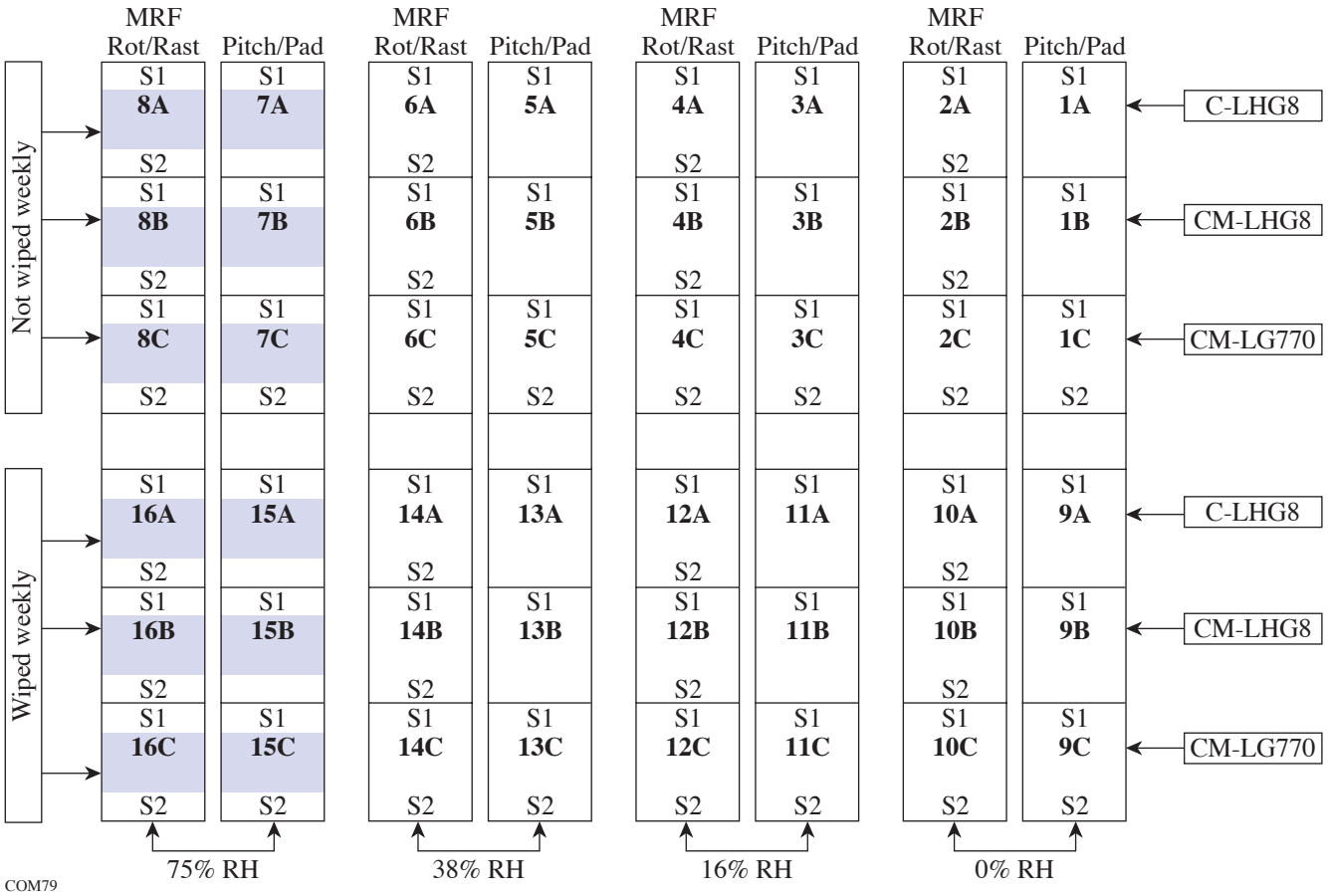

Figure 100.35
Distribution of 48 phosphate glass samples for chemical durability tests (see text).

2. Sample Handling and Storage

Four chambers were set up for the humidity testing. Each chamber maintained a static noncirculating air environment and was kept sealed except during removal and replacement of samples. Temperature in the chambers remained between 21°C and 22°C. Humidities of 0%, 16%, 38%, and 75% (±1%) RH were maintained in the chambers using desiccant (0% RH) and saturated aqueous solutions of LiCl, NaI, and NaCl, respectively. Temperature and humidity were monitored daily using hygrometer/thermometer pens,[11] which remained in the sealed chambers.

Samples were mounted upright in these humidity chambers in foam holders with the prepared surfaces exposed. They remained in the chambers for 14 weeks and were removed only for cleaning, measurement, and inspection. Samples were transported to and from the metrology lab in closed plastic boxes and were handled with nitrile gloves. During cleaning, measurement, and inspection, samples were exposed briefly to lab humidity conditions of between 20% and 60% RH, with an average of 32% RH, and temperatures between 21°C and 22°C.

3. Sample Cleaning

A gentle drag–wipe method with HPLC-grade methanol and lens tissue (Lens SX90 tissue from Berkshire) was chosen as an initial "cleaning" protocol for all surfaces. Although not a rigorous "cleaning" process, wiping was selected as being most likely to preserve the quality of initial surfaces for the ensuing humidity tests. Sample wiping consisted of a pair of orthogonally oriented drag wipes per side. Half of the samples underwent this procedure only once before being placed in the humidity chambers; these samples were designated "not weekly wiped" (NWW). The other half of the samples were wiped in this way prior to being placed in the humidity chambers and then wiped again every week for 13 weeks; these samples were designated "weekly wiped" (WW).

A true aqueous cleaning method involving gentle hand scrubbing was chosen as a more aggressive protocol, which was performed at the conclusion of testing, but only on the samples that had been stored in 75% RH. This protocol was chosen after reviewing existing procedures for cleaning laser glass surfaces.[8] After 14 weeks of storage, half of the samples from the 75%-RH chamber were cleaned with 18-Mohm deionized (DI) water alone, and half were cleaned with DI water and detergent (Micro-90 Microsoap). Each sample was held under running DI water while being scrubbed with synthetic nylon wipes (Miracle Wipes). Detergent was added to the surfaces of some of the samples during this process. After scrubbing, samples were rinsed in a DI water spray for 2 min and then set upright in a laminar flow hood[12] to dry. After evaluation, the samples were stored in 0% RH. After 5 additional weeks, the aqueous cleaning procedure was repeated. These cleaning methods are typical of what would be used on optics going into laser systems.

4. Surface-Evaluation Protocols

Although scatter is the main concern for laser systems, no simple, direct way to measure it on these samples was found in this facility. Four easily performed methods for surface evaluation were chosen: measurement of areal microroughness with and without electronic filtering, power spectral density (PSD) analysis, visual inspection, and microscopic inspection.

Areal microroughness measurements were made using a Zygo NewView 100 white-light interferometer, with a 5× Michelson objective.[13] Areal peak-to-valley (p–v) and root-mean-square (rms) values were obtained over areas of 1.41 mm × 1.05 mm. Measurements were made weekly on samples in the 38%- and 75%-RH chambers, and bi-weekly on samples in the 16%- and 0%-RH chambers for the first 10 weeks. Additional measurements were made on samples in the 75%-RH chamber at 13 weeks and after each aqueous cleaning with and without detergent. An average of measurements from five random sites in characteristic areas of the samples was recorded. Uncharacteristic areas, the center, and the edges of the substrates were avoided. Filtering was used on selected data to observe features in specific spatial-frequency ranges suggested by PSD analysis.

PSD analysis provided more-detailed information about what kinds of structures were contributing to the surface roughness. PSD data were gathered for selected surfaces from the New View 100[13] and plotted using in-house MATLAB codes[14] as power density (nm^3) as a function of spatial frequency (1/nm). With the 5× Michelson objective, information was obtained for structures contributing to roughness at spatial frequencies between ~1×10^{-4} 1/nm and ~4×10^{-7} 1/nm (corresponding to periodicities between ~10 μm and ~2.5 mm). Plotted data were compared to a typical specification for NIF laser disks.[15] Various types of visual inspection were employed. General observations were routinely made with the naked eye in fluorescent room light. Inspections with a fiber-optic light source in a dark room were made after 4 and 11 weeks of storage. At 14 weeks, surfaces were inspected, mapped, and described in writing before and after the first aqueous cleaning with and without detergent. Digital photos of the samples were taken in a darkened room with a flash before

and after the first (14 weeks) and second (19 weeks) aqueous cleanings. Microscopic inspection was carried out using a Nikon research-grade, white-light optical microscope before and after the first aqueous cleaning. Surfaces were observed in reflection using both bright-field and dark-field modes with 5×, 10×, 20×, and 50× objectives.

Results of Humidity Study

Very little change was seen on the majority of the surfaces monitored. After 10 weeks of storage, *no degradation* was seen on any of the samples stored at 38% RH, 16% RH, or 0% RH. The experiment was ended for these samples. Within the 75%-RH chamber, *no degradation was seen on any of the samples that underwent the gentle weekly wiping protocol, and no degradation was seen on any of the samples of CM-LHG8 with or without wiping* throughout the 14 weeks they were stored at elevated humidity. The samples of NWW C-LHG8 in the 75%-RH chamber (samples 7A and 8A; refer to Fig. 100.35) showed minor visible degradation, accompanied by increased rms microroughness and elevated levels of PSD, which was worse on the pitch-polished surface (surface S1 of 7A) than on the MRF-polished ones (surfaces S1 of 8A and S2 of 8A). Both of the samples of NWW CM-LG770 (samples 7C and 8C) in the 75%-RH chamber showed severe degradation, confirming the high degree of humidity sensitivity for this composition.

Degradation on samples of NWW CM-LG770 (samples 7C and 8C) first appeared in the form of large structures at low spatial frequencies, increased rms microroughness, and elevated PSD levels. By 13 weeks of storage, structures had developed at higher spatial frequencies, resulting in increased rms and p–v microroughness and elevated PSD levels at high spatial frequencies. The surfaces had also developed a grainy, highly scattering appearance. Although the quality of the initial surface finish did not affect the rate of degradation in samples of NWW CM-LG770 at 75% RH, the various surface-finishing processes appeared to influence how the degradation formed, with different types of structures appearing on surfaces that had been polished differently.

The following four subsections concentrate exclusively on the results observed for selected samples of all glass compositions *stored at 75% RH* and *not wiped weekly*.

1. Changes in Areal Microroughness

The *initial* rms surface areal microroughness of the phosphate glass samples varied from 0.6 nm to 2.2 nm as a result of the different surface-finishing protocols. In general, for all samples, the pad-polished surfaces were roughest, the pitch-polished surfaces were smoothest, and the MRF-processed surfaces fell somewhere in between. This did not depend on glass type. Variations in microroughness were not indicative of polishing process efficiency but were simply the result of polishing conditions available at the time. An example showing *good* environmental stability is given in Fig. 100.36 [(a) rms, (b) p–v] for NWW CM-LHG8 (samples 7B and 8B) stored at 75% RH. All initial surface microroughness values were below 1-nm rms, though differences in rms surface microroughness were seen between surfaces polished with either pitch (surface S1 of 7B) or MRF (surfaces S1 of 8B and S2 of 8B), with the pitch-polished surfaces being the smoothest. Peak-to-valley values generally overlapped and fell in a range between 10 nm and 30 nm. Microroughness levels remained unchanged after 13 weeks of storage.

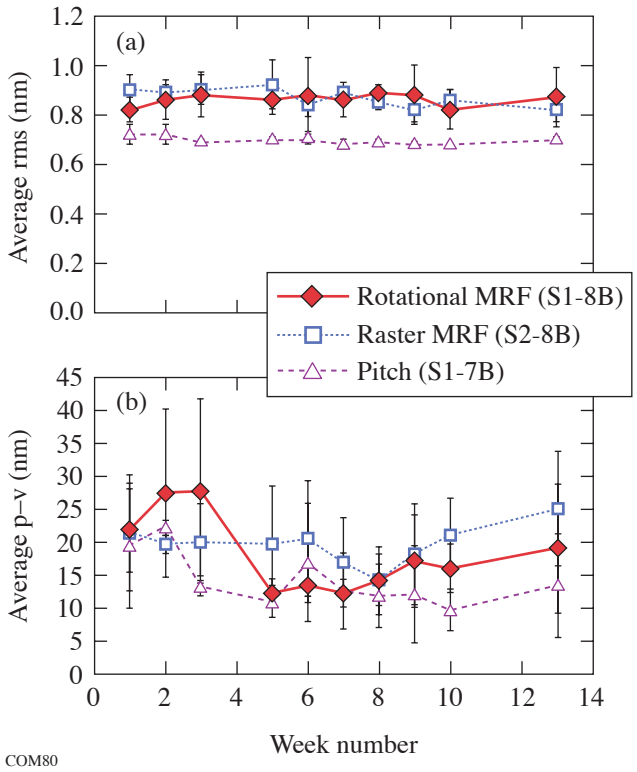

Figure 100.36
Areal microroughness of NWW CM-LHG8 (samples 7B and 8B) surfaces over 13 weeks of storage in 75% RH (lines to guide the eye). (a) Areal rms; (b) areal p–v.

An example showing *moderate* environmental stability is given in Fig. 100.37. No significant changes in either rms or p–v roughness were observed on samples of NWW C-LHG8 (samples 7A and 8A) throughout the first 8 weeks of storage at

75% RH. These samples showed increasing rms and p–v microroughness beginning at week 9 and week 10, respectively. Increases in microroughness continued through 13 weeks of storage [see Figs. 100.37(a) and 100.37(b)]. The increases were much more dramatic for the pitch-polished surface of sample 7A (rms: 3.9 nm±2.5 nm; p–v: 450 nm± 370 nm) than for the two MRF-polished surfaces of sample 8A.

An example of *significant* environmental *instability* is given in Fig. 100.38. Both the rms and p–v roughness values of the two samples of NWW CM-LG770 (samples 7C and 8C) remained stable throughout the first 4 weeks of storage. Measurable increases in rms microroughness on all four surfaces of these samples were detected after 5 to 7 weeks of storage [see Fig. 100.38(a)]. The rms roughness continued to increase on all four surfaces of both samples of NWW CM-LG770 through 10 weeks. These increases in rms roughness were *not* accompanied by increases in p–v roughness [see Fig. 100.38(b)]. By week 13, however, both rms and p–v roughness values had increased dramatically (rms: 8 nm to 24 nm; p–v: 480 nm to 1090 nm). The standard deviations on the week-13 measurements were very large (rms: ± >4.3 nm; p–v: ± >200 nm). There was no direct correlation between the initial surface rms roughness level and rate of degradation. In fact, the pad-polished surface (surface 7C of S2), which was initially the roughest, showed the *smallest* increase in rms roughness values after 13 weeks. The raster MRF-processed surface (surface 8C of S2) showed the greatest increase in rms roughness. The magnitudes of all of the changes on the NWW CM-LG770 surfaces were much greater than those detected on surfaces of any of the LHG8 samples.

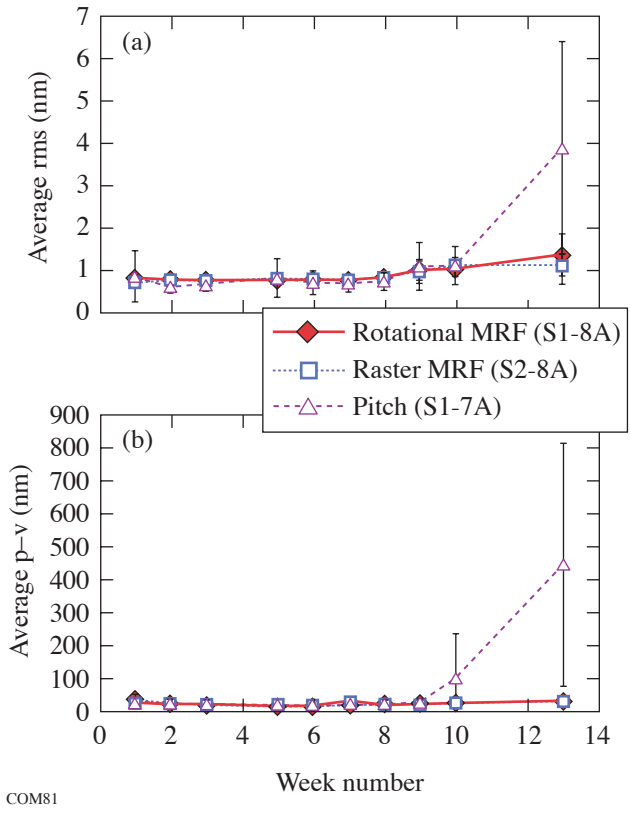

Figure 100.37
Areal microroughness of NWW C-LHG8 (samples 7A and 8A) surfaces over 13 weeks of storage in 75% RH (lines to guide the eye). (a) Areal rms; (b) areal p–v.

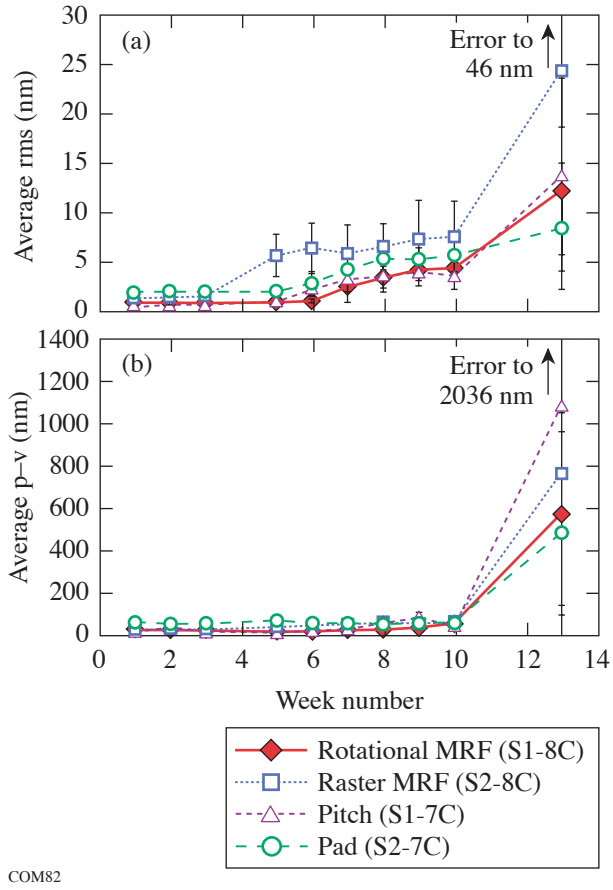

Figure 100.38
Areal microroughness of NWW CM-LG770 surfaces (samples 7C and 8C) over 13 weeks of storage in 75% RH. (a) Areal rms; (b) areal p–v.

2. Analyses of Power Spectral Density

As expected, since the area under a power spectral density (PSD) curve is proportional to the square of the rms,[16] *initial* surface-rms-roughness differences were also reflected in PSD data. Figure 100.39 gives PSD plots for initial surfaces of NWW CM-LHG8 and NWW CM-LG770 (surfaces S1 of 7B, S2 of 7C, S1 of 8B, and S2 of 8B). The pad-polished surface of 7C had the highest power-density levels (pad-polished surfaces were the only surfaces with power-density levels above the NIF specification for laser disks[15]), while the pitch-polished surface of 7B had the lowest. The power-density levels of the two MRF-polished surfaces of 8B were comparable to the pitch-polished surface at high spatial frequencies and rose to levels between the pitch-polished and pad-polished surfaces at low spatial frequencies.

Figure 100.40 shows selected PSD plots for the pitch-polished surface S1 of sample 7A of NWW C-LHG8 stored in the 75%-RH chamber, which was initially well polished and below the NIF reference level. The plot shows that power density increased by two orders of magnitude over all spatial frequencies after 13 weeks of storage. The other two surfaces of NWW C-LHG8 (the rotationally MRF-processed surface S1 of 8A and the raster MRF–processed surface S2 of 8A) showed small increases in power density over 13 weeks. Figure 100.41 shows results for the rotationally MRF-processed surface only. Increases by less than 10× were observed at spatial frequencies between 10^{-4} 1/nm and 10^{-5} 1/nm (periodicities between 10 μm and 100 μm), with no changes observed at lower spatial frequencies (longer periods). (Note: PSD data in Figs. 100.40–100.42 after aggressive aqueous cleaning are discussed in the **Aqueous Cleaning Results…** section, p. 265.)

All four surfaces of the two samples of NWW CM-LG770 (7C and 8C) showed significant increases in levels of power density between 5 weeks and 7 weeks. Figure 100.42 shows selected PSD plots for the rotationally MRF-processed surface S1 of 8C. At week 10 (not shown), power density at low spatial

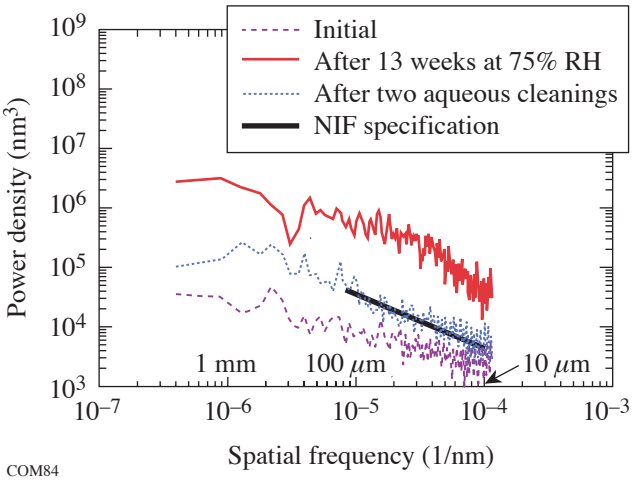

Figure 100.40
Selected PSD data for a pitch-polished surface of NWW C-LHG8 (S1 of 7A) stored in 75% RH for 13 weeks.

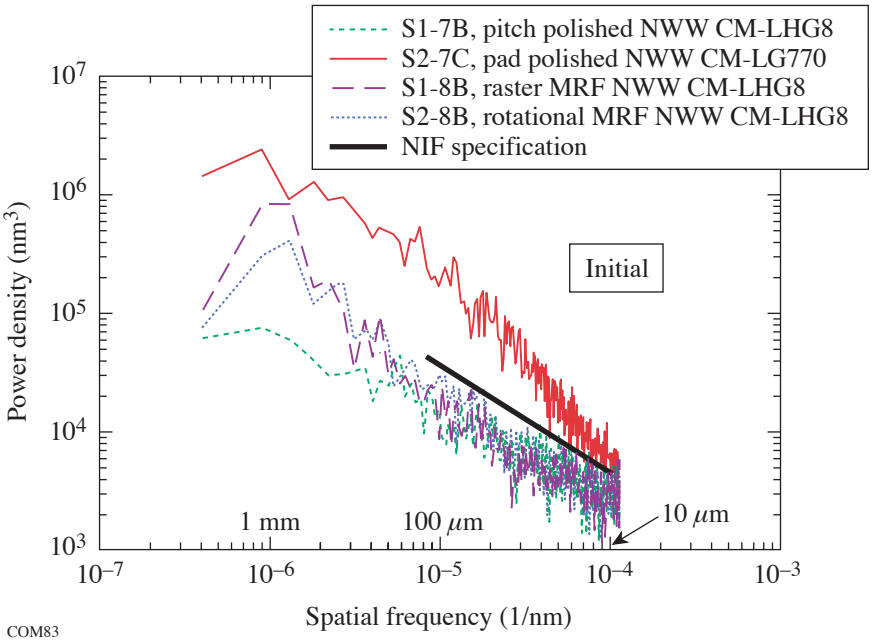

Figure 100.39
PSD plot of different initial surface finishes of NWW CM-LHG8 and NWW CM-LG770 before storage in 75% RH.

frequencies (2×10^{-6} 1/nm to 4×10^{-7} 1/nm) had increased by ~15×, while at higher spatial frequencies the departure from the initial condition was less. By week 13, power-density levels at middle-to-high spatial frequencies had also increased significantly, with a "bump" in the data around a spatial frequency of 5×10^{-5} 1/nm (corresponding to a periodicity of 20 μm; see Fig. 100.42).

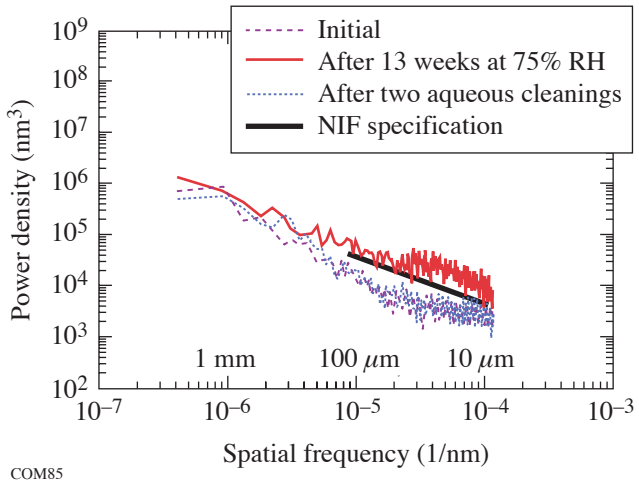

Figure 100.41
Selected PSD data for a rotationally MRF-processed surface of NWW C-LHG8 (S1 of 8A) stored in 75% RH for 13 weeks.

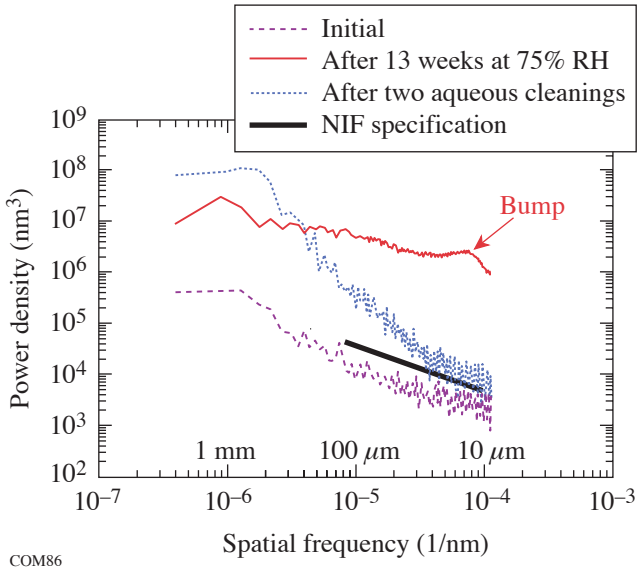

Figure 100.42
Selected PSD data for a rotationally MRF-processed surface of NWW CM-LG770 (S1 of 8C) stored in 75% RH for 13 weeks.

Rising PSD levels on S1 of 8C (see Fig. 100.42) corresponded to surface features observed with white-light interferometry. Increased power density at lower spatial frequencies correlated with large surface features that are best described as "mottling." Figure 100.43 shows this mottling as viewed with the NewView 100 using a low-pass filter (333 μm). By week 13, small structures varying in size from 4 μm to 50 μm in diameter, as measured by optical microscopy, had also developed on the surface. The size of the larger of these structures (>10 μm) corresponds to the "bump" in the PSD plot for week 13. Structures with sizes in the middle spatial frequencies (1×10^{-5} 1/nm to 4×10^{-6} 1/nm) also appeared by week 13. Figure 100.44 shows these structures viewed on the white-light interferometer using a bandpass

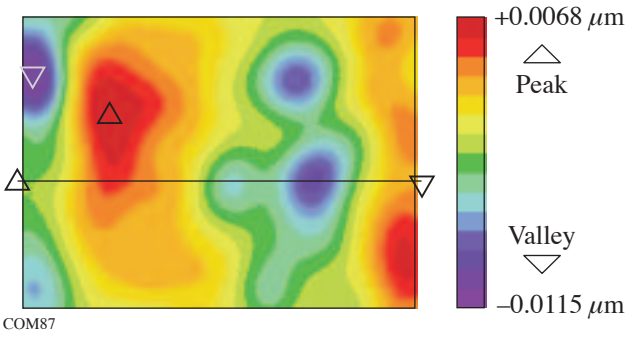

Figure 100.43
NewView 100 grayscale image of structures at low spatial frequencies on rotationally MRF-processed NWW CM-LG770 (S1 of 8C), stored in 75% RH for 13 weeks, viewed with a 333-μm, low-pass filter. 1.41-mm × 1.05-mm areal view. p–v: 18.4 nm; rms: 3.44 nm.

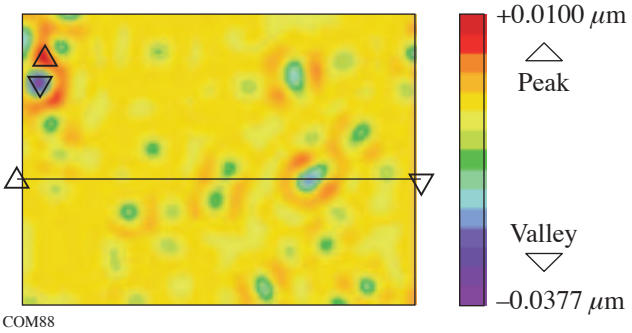

Figure 100.44
NewView 100 grayscale image of structures at middle-range spatial frequencies on rotationally MRF-processed NWW CM-LG770 (S1 of 8C), stored in 75% RH for 13 weeks, viewed with a 100- to 250-μm bandpass filter. 1.41-mm × 1.05-mm areal view. p–v: 55.6 nm; rms: 3.51 nm.

filter (100 μm to 250 μm). The increased power-density levels at middle-range spatial frequencies for week 13 (see Fig. 100.42) show that they make a significant contribution to increased rms roughness.

3. Visual Inspection

Visual inspection at 11 weeks and beyond agreed in general with more quantitative optical measurements. The presence of films, haziness, and graininess could be correlated to samples that had shown increases in microroughness and PSD levels. In some cases, visual inspection revealed differences among parts that were not measurable with metrology instrumentation, presumably because the human eye is more sensitive to scatter than the metrology instruments we used. Surfaces of some of the MRF-processed parts looked better than those of the pitch-polished and pad-polished ones, and surfaces on the samples of CM-LHG8 looked better than surfaces on the samples of C-LHG8. At the conclusion of 14 weeks of exposure, there was considerable particulate contamination and a "busy" appearance on many surfaces.

4. Microscopic Inspection

Microscopic inspection after 14 weeks of storage was useful for evaluating significantly degraded surfaces prior to aggressive cleaning and for observing structures with high spatial frequencies that developed on the surfaces. These structures varied in both size (4 μm to 50 μm in diameter) and appearance from surface to surface. We attribute these variations to the different initial finishing processes used and any residual contaminants unique to each finishing process that may have been left on each surface. The pitch-polished surface of NWW C-LHG8 (S1 of 7A) was covered in ran-domly distributed, nominally round features that were 8 μm to 12 μm in diameter, as seen in bright field mode using a 20× objective. These features are shown in Fig. 100.45(a). The pitch-polished surface of NWW CM-LG770 (S1 of 7C) was also covered in nominally round features that were smaller (about 4 μm in diameter) than those on the NWW C-LHG8 surface. The pad-polished surface of NWW CM-LG770 (S2 of 7C) showed oblong and elevated features that were ~4 μm wide and 8 μm to 16 μm long. The MRF-processed surfaces of NWW CM-LG770 (S1 of 8C and S2 of 8C) had asymmetrical, elevated features between 10 μm and 40 μm in diameter that resembled snowflakes. On the rotationally MRF-processed surface (S1 of 8C), these features were isolated from other defects, as shown in Fig. 100.46. On the raster-polished surface (S2 of 8C), the snowflake-like features appeared to surround some of the numerous dark, round artifacts that covered the surface (see Fig. 100.47). This finding suggests that the dark, round artifacts are defects (possibly residual contaminant from the polishing process) that act as initiation sites for degradation, as reported in previous work.[1]

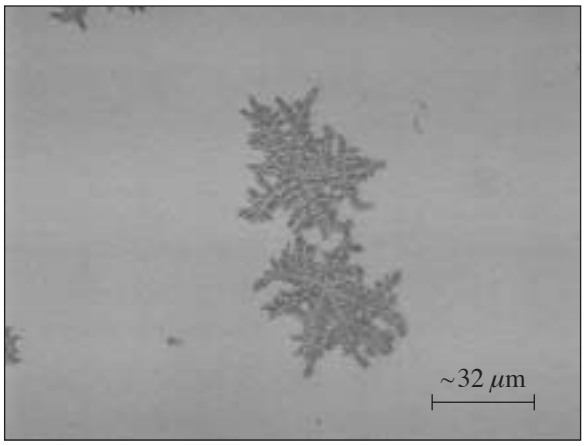

COM90

Figure 100.46
Optical microscope image of rotationally MRF-processed NWW CM-LG770 (S1 of 8C) after 14 weeks of storage at 75% RH, before cleaning, viewed in bright field at 50×.

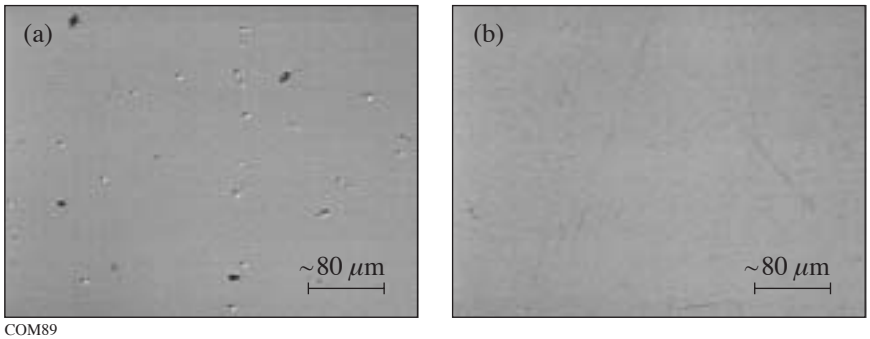

COM89

Figure 100.45
Optical microscope images of pitch-polished NWW C-LHG8 (S1 of 7A) at 14 weeks, before (a) and after (b) aqueous cleaning, viewed in bright field at 20×.

Aqueous Cleaning Results for All Samples Stored at 75% RH

More-aggressive cleaning protocols were employed at the conclusion of the 14-week humidity test to determine how readily degraded surfaces could be restored, to evaluate the permanence of degradation observed, and to evaluate the effects of aqueous cleaning on "good" surfaces. Because no differences were observed between the results for samples cleaned with DI water alone and those cleaned with DI water and detergent, in the following discussion we do not differentiate between the two aqueous cleaning protocols.

Initial aqueous cleaning visibly improved the appearance of all WW and NWW surfaces by removing films and particulates. All of the 4-μm to 50-μm structures observed microscopically [see Figs. 100.45(a), 100.46, and 100.47) were removed by a single cleaning. For NWW surfaces that exhibited degradation, this single cleaning removed surface structures that developed at high spatial frequencies, and it reduced the number density of surface structures that developed at middle-range spatial frequencies. It did not remove any of the low-spatial-frequency structures that developed on some surfaces.

A second aqueous cleaning did not further improve, and in some cases damaged, the surfaces. Both first and second cleanings generated hazing (that was visible to the naked eye) due to scratching (that was visible microscopically) on pitch-polished and pad-polished surfaces of NWW and WW samples of all glass types [as shown for surface S1 of 7A in Fig. 100.45(b)]. The microscopic scratches are believed to be caused by subsurface damage from finishing and not by cleaning. During cleaning, these scratches become enlarged (along with other defects) by water-induced corrosion of the glass surface.[7,17] Considerably less hazing and scratching were observed on the MRF-processed surfaces. We attribute this improved quality to the ability of MRF to both polish without creating subsurface damage and to remove subsurface damage from previous processing.[18] These obvious visible changes were only modestly supported by measured changes in areal rms roughness and power-density levels, as discussed below.

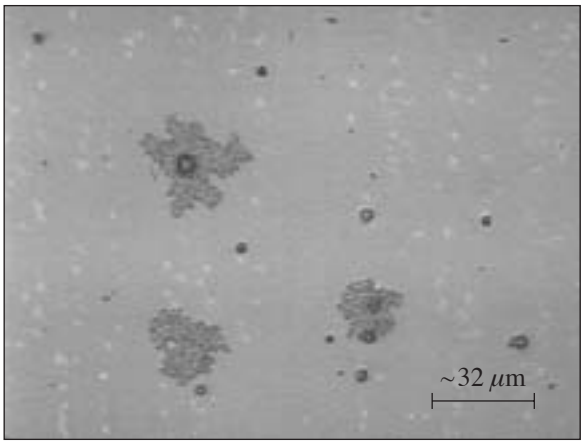

COM91

Figure 100.47
Optical microscope image of raster MRF-processed NWW-LG770 (S2 of 8C) after 14 weeks of storage at 75% RH, before cleaning, viewed in bright field at 50×.

Areal *p–v microroughness* was reduced to below initial levels on *WW surfaces of all glass types* after one aqueous cleaning. This finding indicates that the drag–wiping protocols performed on the samples before the experiment began were insufficient to rid the surfaces of debris remaining from the various finishing processes. One application of the more-aggressive aqueous cleaning process was sufficient to remove most of this debris. After a second aqueous cleaning, areal p–v values remained unchanged. *NWW surfaces of C-LHG8 and CM-LHG8* behaved similarly, exhibiting areal p–v levels reduced to below initial values after one aqueous cleaning, and these remained unchanged after a second aqueous cleaning. Cleaning was not as effective *on NWW surfaces of CM-LG770*. After one aqueous cleaning, these surfaces exhibited p–v values below those at 13 weeks, but still higher than initial. After a second aqueous cleaning, areal p–v generally increased on these surfaces.

Changes in *rms microroughness* for all *NWW* parts stored at 75% RH are given in Table 100.I. After the first aqueous cleaning, surfaces of CM-LHG8 were unchanged from what they were at the beginning of the experiment. Most surfaces of C-LHG8 and CM-LG770 samples showed significant improvement from their degraded (week 13) states. Areal roughness was reduced by 18% to 74%. All CM-LG770 surfaces were still much rougher than they had been at the beginning of the experiment. A second cleaning did not further reduce roughness. For seven out of ten surfaces, rms-roughness levels increased.

Changes in the rms-microroughness values on NWW samples after aqueous cleaning were reflected in the PSD data. On the pitch-polished sample of NWW C-LHG8 (S1 of 7A), two aqueous cleanings uniformly lowered power density over all spatial frequencies; however, they did not return the surface to its initial condition, as can be seen in Fig. 100.40. After two aqueous cleanings, areal rms roughness and PSD levels were

returned to their initial conditions for the MRF-processed surfaces of NWW C-LHG8 (S1 of 8A and S2 of 8A) (shown in Fig. 100.41).

On samples of NWW CM-LG770, different spatial-frequency regions were affected differently by aqueous cleaning. PSD data for the rotationally MRF-processed surfaces of NWW CM-LG770 (S1 of 8C) are shown in Fig. 100.42. Structures at high- and middle-range spatial frequencies were significantly reduced. Aqueous cleaning did not reduce structures at low spatial frequencies. Power density actually *increased* at spatial frequencies between 3×10^{-6} 1/nm and 4×10^{-7} 1/nm, which explains why rms-microroughness values remained high.

Changes in *rms microroughness* for all *WW* parts stored at 75% RH are given in Table 100.II. After the first aqueous cleaning, 6 of 10 surfaces were brought to a level equal to or better than that measured at the beginning of the experiment. *All* six of these surfaces had been processed with MRF. Most of the MRF-processed surfaces continued to improve after a second cleaning. Results were mixed for the surfaces that had been pitch polished or pad polished.

Summary/Conclusions

No samples of LHG8 (cast/continuously melted) or LG770 (continuously melted) exhibited any change after 10 weeks of exposure at 21°C to humidity at 38% RH or less. Changes *were* seen on *some* of the samples stored in 75% RH at 21°C, and several conclusions can be made regarding the sensitivity to humidity and cleaning of well-polished (with rms microroughness below 2 nm) LHG8 and LG770 surfaces exposed to these conditions.

Among glass types:

1. Continuously melted LHG8 is more resistant to humidity-induced degradation than cast LHG8. Continuously melted LHG8 surfaces exhibit no degradation after 14 weeks of exposure, while cast LHG8 surfaces exhibit little to moderate degradation.
2. Continuously melted LG770 surfaces exhibit severe degradation after 14 weeks of exposure, indicating that continuously melted LG770 is much more sensitive to humidity than either type of LHG8.

Table 100.I: Areal rms microroughness of NWW samples after aqueous cleaning. Percent changes in roughness after each cleaning are noted.

NWW rms (nm)		Initial (week 0)	Final (week 13)	After First Cleaning (week 14)	After Second Cleaning (week 19)
C-LHG8	S1 of 7A (pitch)	0.63±0.15	3.89±2.50	1.02±0.12 (–74%)	1.75±0.94 (+72%)
	S1 of 8A (rot MRF)	0.79±0.07	1.38±0.50	1.10±0.19 (–20%)	0.89±0.07 (–19%)
	S2 of 8A (rast MRF)	0.78±0.05	1.13±0.41	0.93±0.10 (–18%)	0.98±0.16 (+5%)
CM-LHG8	S1 of 7B (pitch)	0.72±0.04	0.70±0.01	0.70±0.01 (+0%)	0.78±0.01 (+11%)
	S1 of 8B (rot MRF)	0.86±0.08	0.87±0.12	0.84±0.16 (–3%)	0.80±0.08 (–5%)
	S2 of 8B (rast MRF)	0.89±0.03	0.82±0.05	0.80±0.02 (–2%)	0.92±0.14 (+15%)
CM-LG770	S1 of 7C (pitch)	0.70±0.01	13.84±9.72	5.93±1.16 (–58%)	7.59±3.08 (+28%)
	S2 of 7C (pad)	2.05±0.34	8.41±4.31	9.61±3.06 (+14%)	12.51±5.97 (+30%)
	S1 of 8C (rot MRF)	0.91±0.08	12.21±6.43	9.87±3.24 (–19%)	16.68±13.21 (+69%)
	S2 of 8C (rast MRF)	1.46±0.11	24.26±21.95	13.51±5.00 (–44%)	10.01±2.30 (–26%)

Table 100.II: Areal rms microroughness of WW samples after aqueous cleaning. Percent changes in roughness after each cleaning are noted.

WW rms (nm)		Initial (week 0)	Final (week 13)	After First Cleaning (week 14)	After Second Cleaning (week 19)
C-LHG8	S1 of 15A (pitch)	0.71±0.07	0.74±0.10	0.76±0.06 (+3%)	0.74±0.03 (–3%)
	S1 of 16A (rot MRF)	0.84±0.15	0.90±0.25	0.73±0.04 (–19%)	0.72±0.05 (–1%)
	S2 of 16A (rast MRF)	0.84±0.07	1.02±0.32	0.82±0.08 (–20%)	0.76±0.07 (–7%)
CM-LHG8	S1 of 15B (pitch)	0.72±0.03	0.77±0.06	0.86±0.02 (+12%)	0.93±0.02 (+8%)
	S1 of 16B (rot MRF)	0.89±0.05	1.05±0.12	0.81±0.04 (–23%)	0.79±0.09 (–2%)
	S2 of 16B (rast MRF)	0.98±0.07	0.88±0.06	0.86±0.06 (–2%)	0.86±0.02 (+0%)
CM-LG770	S1 of 15C (pitch)	0.72±0.03	0.76±0.07	0.98±0.08 (+29%)	1.18±0.18 (+22%)
	S2 of 15C (pad)	1.56±0.11	1.34±0.09	1.72±0.20 (+28%)	1.66±0.05 (–3%)
	S1 of 16C (rot MRF)	0.94±0.07	1.74±1.93	0.91±0.07 (–48%)	0.89±0.11 (–2%)
	S2 of 16C (rast MRF)	1.38±0.19	1.38±0.08	1.38±0.15 (+0%)	1.38±0.19 (+0%)

3. Aqueous cleaning can improve surfaces of cast LHG8 and continuously melted LG770 after *severe degradation* by humidity, but it cannot return them to their original conditions. (Aqueous cleaning of degraded continuously melted LG770 surfaces can significantly reduce structures at high- and middle-range spatial frequencies, but it is not effective at removing large structures at low spatial frequencies.)

For all glass types:

4. There is no clear correlation between initial finished surface quality (among surfaces with better-than-2-nm-rms microroughness) and quantifiable magnitude of degradation due to humidity; however, different surface structures develop on surfaces finished with different processes.
5. Gentle weekly drag wiping with methanol prevents humidity-induced degradation.
6. A single aqueous cleaning is sufficient to remove debris from polishing remaining on glass surfaces after gentle drag wiping and storage for 14 weeks.
7. One or two aqueous cleanings can cause increased haze from microscopic scratches on surfaces finished with pitch or pads.
8. MRF processing ensures that at least two aqueous cleanings can be performed to remove debris, without risk of increasing surface haze from microscopic scratches. We attribute this result to the low levels of subsurface damage remaining on surfaces after MRF processing.

ACKNOWLEDGMENT

The authors thank H. Romanofsky of the Center for Optics Manufacturing at the University of Rochester for MRF processing of the samples. We thank A. Maltsev of LLE for pitch polishing and G. Kowski and G. Mitchell of LLE for sample cleaning, inspection, and microscopy. The idea for this work was prompted by an internal poster paper prepared by P. Ehrmann and J. Campbell of LLNL and made available to J. Kelly of LLE in January 2004. The authors acknowledge the Laboratory for Laser Energetics at the University of Rochester for continuing support. One of the authors (JD) is an LLE Horton Fellow. This research was also supported by the U.S. Department of Energy (DOE) Office of Inertial Confinement Fusion under cooperative agreement DE-FC52-92SF19460, the University of Rochester, and the New York State Energy Research and Development Authority. The support of the DOE does not constitute an endorsement by the DOE of the views expressed in this article.

REFERENCES

1. T. I. Suratwala *et al.*, in *Optical Engineering at the Lawrence Livermore National Laboratory II: The National Ignition Facility*, edited by M. A. Lane and C. R. Wuest (SPIE, Bellingham, WA, 2004), Vol. 5341, pp. 102–113.

2. Laboratory for Laser Energetics LLE Review **96**, 207, NTIS document No. DOE/SF/19460-509 (2003). Copies may be obtained from the National Technical Information Service, Springfield, VA 22161.

3. D. C. Brown, S. D. Jacobs, J. A. Abate, O. Lewis, and J. Rinefierd, in *Laser Induced Damage in Optical Materials: 1977*, edited by A. J. Glass and A. H. Guenther, Natl. Bur. Stand. (U.S.), Spec. Publ. 509 (U.S. Government Printing Office, Washington, DC, 1977), pp. 416–422.

4. W. Seka, J. Soures, O. Lewis, J. Bunkenburg, S. Jacobs, G. Mourou, J. Zimmermann, and D. Brown, Appl. Opt. **19**, 409 (1980).

5. J. H. Campbell *et al.*, J. Non-Cryst. Solids **263–264**, 342 (2000).

6. T. I. Suratwala *et al.*, "Polishing Slurry Induced Haze on Phosphate Laser Glasses," to be submitted to the Journal of Non-Crystalline Solids.

7. "Staining and Dimming in Polishing Process," Technical Report No. HGW-0-6904E, Hoya Glass Works, Ltd. (1970).

8. "Receive, Clean, Inspect, and Package Laser Amplifier Slabs," NIF Operations Procedure No. NIF50100570A, Lawrence Livermore National Laboratory, Livermore, CA (2002).

9. D. Golini, S. Jacobs, W. Kordonski, and P. Dumas, in *Advanced Materials for Optics and Precision Structures*, edited by M. A. Ealey, R. A. Paquin, and T. B. Parsonage, Critical Reviews of Optical Science and Technology (SPIE, Bellingham, WA, 1997), Vol. CR67, pp. 251–274.

10. J. E. DeGroote, H. J. Romanofsky, I. A. Kozhinova, J. M. Schoen, and S. D. Jacobs, in *Manufacturing and Testing V*, edited by H. P. Stahl (SPIE, Bellingham, WA, 2004), Vol. 5180, pp. 123–134.

11. VWR Humidity/Temperature Pen with Memory, VWR Catalog No. 35519-049, VWR Scientific, St. Paul, MN 55121.

12. Horizontal laminar flow hood, surpasses Class 100 conditions, Dexon Manufacturing, Inc., Rush City, MN 55069.

13. Zygo NewView™ 100 Settings—Filter: Off; Remove: Cylinder; Remove Spikes: Off; Min Mod: 5%; Scan Length: 20-μm bipolar; FDA Res: High; Min Area Size: 7.

14. J. E. DeGroote, S. N. Shafrir, J. C. Lambropoulos, and S. D. Jacobs, presented at The 88th OSA Annual Meeting, Rochester, NY, 10–14 October 2004.

15. Specification taken from LLNL/NIF Drawing No. AAA96-105113, Lawrence Livermore National Laboratory, Livermore, CA.

16. E. L. Church, in *Precision Surface Metrology*, edited by J. C. Wyant (SPIE, Bellingham, WA, 1983), Vol. 429, pp. 105–112.

17. T. Izumitani *et al.*, in *The Science of Ceramic Machining and Surface Finishing II*, edited by B. J. Hockey and R. W. Rice, Natl. Bur. Stand. (U.S.), Spec. Publ. 562 (U.S. Government Printing Office, Washington, DC, 1979), pp. 417–425.

18. J. A. Menapace *et al.*, in *Laser-Induced Damage in Optical Materials: 2001*, edited by G. J. Exarhos *et al.* (SPIE, Bellingham, WA, 2002), Vol. 4679, pp. 56–68.